

Internally oxidized Ag-based alloys; the passivation and the influence of chemical composition

Ph.D.Ph.D. Jožica Bezjak A. Professor

Abstract—The aim of this work was to analyse the mechanisms of hindered internal passivation of silver based alloys which was obtained by the modification of basic chemical composition. A generalisation of the phenomenon, experimental verification and the estimated range of micro-element concentration is also introduced. The ability for inoculation of a particular alloy is determined by the differences between the formation energies of oxides, as well as their crystallographic similarity. Therefore, for the investigated Ag-Zn alloys, Mg was selected as the micro-alloying element. The influence of 0.001 up to 0.5 mass % of Mg added to the selected alloys was analysed. By changing the chemical composition, internal passivation was hindered, internal oxidation rate was increased, and considerably greater (redoubled) depths of internal oxidation were achieved.

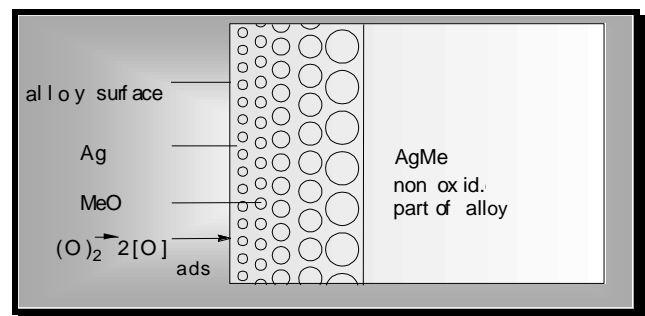
Keywords - internal oxidation, modification, hindrance of passivation

1 INTRODUCTION

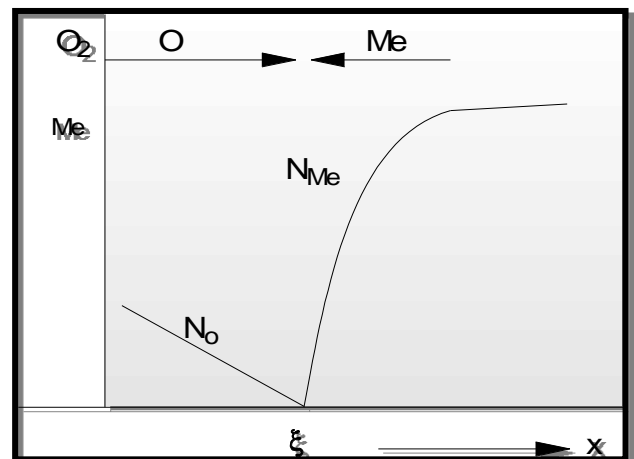
Ag, Cu and Ni based alloys with small additions of noble alloying elements like indium, tin, and antimony oxidise internally if they are exposed to oxidation atmosphere at elevated temperatures. For internal oxidation of a particular alloy, the following conditions also have to be fulfilled:

- the base metal must have high solubility of oxygen
- the alloying element has to be strongly electronegative
- the diffusion rate of oxygen into the base metal has to be of some levels of magnitude higher than the diffusion rate of the alloying elements
- the concentration of the alloying elements has to be inside certain limits
- sufficient partial pressure of oxygen has to be ensured in the atmosphere

If the selected alloy is isothermally annealed at an elevated temperature and all other above mentioned conditions are fulfilled, dissolution of oxygen begins on the surface of the alloy, and its diffusion into the interior, as well as its reaction with atoms of the alloying element occurs. The effect of the oxidation reaction is a precipitation of the finely dispersed oxide of the less noble component in the metal matrix (Pictures 1a and



Picture 1a: the effect of oxidation reaction



Picture 1 a, b: Concentration gradient of oxygen and the alloying element in the zone of internal oxidation, as well as in the non-oxidised part of the alloy⁽¹⁾.

Ph.D..Ph.D. Jožica Bezjak A. Professor, University of Primorska, PEF, President of Association of Technical Creativeness Educators Slovenia.

2 EXPERIMENTAL WORK

In internally oxidised Ag based alloys, where passivation normally occurs, we tried to hinder passivation with small modifications of chemical composition. The hindrance of passivation, undisturbed oxidation of the main alloying element and growth of the internal oxidation zone were obtained with small additions of micro-alloying elements (from 0.001 up to 0.5 mass %) which possess very large free energy of oxide formation. During the selection of the alloys chemical composition, the following criteria were taken into consideration:

- the selected Ag based alloys are mono-phased
- the concentration of the main alloying element is approximately half the critical one ($N_{Me}^{(3)}$)
- on the basis of the Ag-Zn binary phase diagram and relatively small free formation energy for ZnO, Zn was selected as the main alloying element
- in the investigated binary alloying system (Ag-Zn), the added micro-alloying element has very large free oxide formation energy in comparison with the free oxide formation energy of the main alloying element
- the concentrations of added Mg were relatively small (between 0.5 and 0.001 mass %); therefore, this element is designated as a micro-alloying element
- inoculation with Mg was analysed from two standpoints: differences in free formation energy of oxides and appropriate crystallographic features with regard to the silver matrix (**Table 1**).

On the basis of the above mentioned criteria, the selected Ag-Zn and Ag-Zn-Mg are given in **Table 2** for observation of the passivation phenomenon and the conditions for its hindrance.

Table 1:

Consecutive number	Basic metal	Master alloying element Zn Mg	Second alloying element Mg	Alloy designation
		mass % (at.%) mass % (at.%)	mass % (at.%)	
1	Ag	6.3 (9.97)		2S1
2	Ag	0.045 (0.20)		2S0
3	Ag	5.8 (9.18)	0.51 (2.29)	3S1
4	Ag	5.8 (9.18)	0.29 (1.31)	3S2
5	Ag	5.0 (7.91)	0.26 (1.18)	1S4
6	Ag	5.8 (9.18)	0.21 (0.95)	2S2
7	Ag	5.8 (9.18)	0.065 (0.29)	2S3
8	Ag	5.8 (9.18)	0.012 (0.05)	3S3
9	Ag	5.0 (7.91)	0.001 (0.005)	1S6
10	Ag	5.8 (9.18)	<0.002 (0.009)	2S4
11	Ag	5.8 (9.18)	0.001 (0.005)	3S4

temperature and to prevent oxidation of Mg. Alloys were melted inductively in evacuated (10^{-2} bar) quartz tubes. The melting temperature of alloys was approximately 1,050°C. The castings were annealed in quartz tubes at homogenisation temperature of 800°C for 30 hours. Then, the annealed castings were hot forged into small 5 mm thick plates. These plates were then recrystallization annealed for 10 minutes at 750°C and additionally thinned with cold rolling into 0.1 mm thick and 3 mm wide ribbons. From these, plates of different sizes were then cut out (plate length $\approx 3 \times$ plate thickness). The plates were also surface ground and etched in 10 % aqueous solution of nitrous acid (HNO_3) for 10 to 20 seconds.

Table 2:

Base metal	1.1.1.1.1 Oxide of main alloying element							literature
	Oxide	Crystal system	Structure type	Space group	Molar volume (cm^3)	a (nm)	ΔG (kJ/mol) at 800°C	
Ag								(7)
a=0.409nm	ZnO	hexagonal	B4	P6 ₃ mc	14.2	0.421	-243	
Oxide	1.1.1.1.2 Oxide of second alloying element							literature
	Oxide	Crystal system	Structure type	Space group	Molar volume (cm^3)	a (nm)	ΔG (kJ/mol) at 800°C	
Ag ₂ O								(7)
Molar vol. 32.1 cm ³	MgO	cfc	B1	Fm3m	11.25	0.421	-483	

2.1 Preparation and heat treatment of alloys

The alloys were prepared from pure metals: Ag, Zn and Mg (all with purity 99.99 %). Mg was added in the form of Ag-Mg pre-alloy. It was wrapped in a Zn foil and placed into a test tube. Then, the test tube was put into the region with Zn redundancy in order to melt the pre-alloy at a lower

Internal oxidation experiments were performed at different temperatures (in the temperature range between 750°C and 850°C) and for different times (from 5 to 140 hours) in a tube furnace with a 5 cm long, relatively uniform heating zone. Inside this zone, the temperature variation was $\pm 3^\circ\text{C}$ maximum, depending on oxidation temperature. Temperatures were measured by Ni-NiCr thermocouples at the heating elements and directly above the samples in the furnace heating zone. In most cases, air was used as the oxidation atmosphere. An air pump ensured forced circulation of the air. Some experiments were also performed in oxygen atmosphere with partial oxygen pressure of 1.01×10^5 Pa. After oxidation, samples were cut perpendicular to the oxidised zone and then standard metallographic sample preparation was performed for microstructural investigation. Vickers hardness (HV_2) along the cross-section of samples was also determined.

2.2 Investigations of oxidised alloys

Distribution of Zn and Mg was determined by the EMPA (Electron Micro-Probe Analyser). With line and spot analysis, the alloying elements distribution of internally oxidised and homogenised samples was estimated. Microstructural changes of internally oxidised samples were observed and determined by the optical and scanning electron microscope (SEM). The standard metallographic sample preparation was performed. Polished and etched samples were then observed with the optical microscope. The preparation of the samples for TEM (Transmission Electron Microscopy) investigations was as follows:

- thin 20 μm plates were prepared by cutting and mechanical grinding
- subsequent thinning of samples was performed by ionic etching

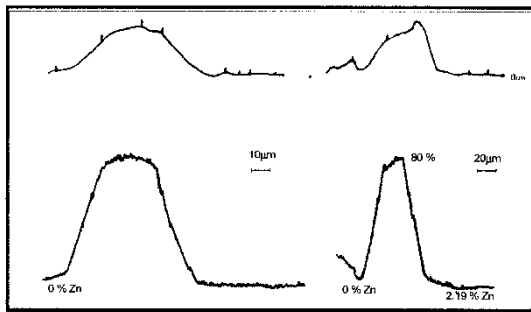
High density and small divergence of ion beam with energy of 4 keV made it possible to etch samples at very small angles of incidence (with regard to the basal plane). The samples oscillated during etching in such a manner that the layer was perpendicular to the ion beam. With this, lateral etching of the

layer was prevented. The angle of etching was below 7° and, in the last phase of etching, only about 4°. One gun etching, alternating from both sides, was performed.

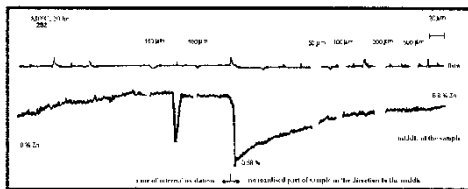
The highest etching rate was obtained at angles of incidence between 60 and 70°; however, a very rough surface of samples was obtained. A smooth surface of samples was obtained at 95° and 87° (measured from the vertical line to the basal plane).

3 RESULTS AND DISCUSION

The concentration distribution of Ag, Mg and Zn in the zone of internal oxidation and in the non-oxidised part of the alloy was determined by EMPA. In the zone of internal oxidation and in its surroundings, the concentration profile of Zn was determined also by EMPA. For the investigations, an Ag-Zn binary alloy (Pic 2), as well as Ag-Zn alloys micro-alloyed with Mg (pic. 3) were selected. With micro-alloying, a homogeneous distribution of fine oxide grains in a metal matrix was obtained.



Picture 2: Zn concentration gradient across the oxide barrier for sample 2S1.



Picture 3: Zn concentration gradient across the zone of internal oxidation and across the non-oxidised part for the sample 2S2 (micro-alloyed with 0.21% of Mg).

The average concentration of Zn in the 2S1 alloy was 6.3%. For this alloy, in the oxide barrier, at the front of the internal oxidation zone, 80% concentration of Zn was determined, and in basic metal, 2.19 % of Zn was dissolved, at the boundary with the internal oxidation zone. In the modified 2S2 alloy, the measured concentration profile of Zn shows that Zn distribution is more uniform than in the 2S3 alloy. In modified alloy, areas with slightly higher concentration of Zn were noticed. This Zn formed an oxide located at the grain boundaries, and other defects were also present in the alloys. This indicates that insufficient micro-alloying was attained. High density and small divergence of the ion beam with energy of 4 keV made it possible to etch samples at very small angles of incidence (with regard to the basal plane). The samples oscillated during etching in such a manner that the layer was perpendicular to the ion beam. With this, lateral etching of layer was prevented. The angle of etching was smaller than 7°, and in the last phase of etching only about 4°. One gun etching, alternating from both sides was performed. The enrichment factor at the front of internal oxidation was 1.25 for the 2S1 alloy and 1.35 for the 2S3 alloy. The average enrichment in the zone of internal oxidation was 1.25. For both alloys, the concentration profile of Zn is symmetrical with regards to the middle of the sample and the concentration of Zn increases towards the front of the internal oxidation zone. The differences obtained by plane geometry measurements were 6-9 %. The depth of the alloying elements' flow zone is very large. In some cases, it is even larger than the depth of the internal oxidation zone. A larger discrepancy was established for the insufficiently micro-alloyed 2S3 alloy, where a higher concentration of Zn (compared to the average one) in the zone of internal oxidation was determined. Zn distribution in the zone of internal oxidation was non-uniform and it can be expected that with prolonged annealing time and increased temperature, the oxide barrier formed in the interior of the sample would hinder further internal oxidation. Microstructural changes in the zone of internal oxidation were observed by optical and electron microscopy. In Ag-Zn alloys, depending on temperature and partial pressure of O₂, either undisturbed oxidation is carried out or continuous oxide barriers are formed. These oxide barriers signal that internal passivation has occurred (Pic 4). Oxide particles are distributed in crystal grains of the Ag matrix. At oxidation temperatures below 800°C (Pic 5), precipitation of oxides at grain boundaries was noticed. The precipitation portion increases with decreased temperature. For the binary alloy Ag-Zn, in the zone of internal oxidation, the precipitation of ZnO in the form of very fine particles (1-5µm), larger needles, whiskers, larger polyhedrons and other irregular particles, as well as lamellas of different sizes oriented parallel to the surface of sample (Pic 6) was noticed. These lamellas, formed from stringers of polyhedrons, are partially disconnected at a fixed depth from the surface, along the whole cross section of the sample and they strongly

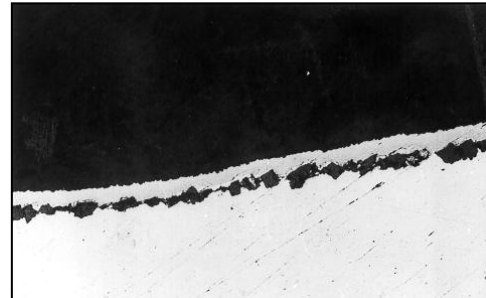
change the morphology of the internal oxidation zone (Pic 7). In the alloys micro-alloyed with Mg, passivation can be inhibited if the concentration of Mg is inside certain limits (Pictures 10 and 11). The main features of such alloys are very fine oxide particles and different defective forms of oxides, which is manifested in an increased concentration of oxides located at the grain boundaries and inside the grains (Pic 6). Characteristic forms are either lamellar folds with certain orientation of oxide lamellas, or a completely irregular distribution of irregularly formed oxides. On the other hand, because of areas with high concentration of oxides, the areas of Ag matrix with either very small concentration of oxides or completely without them are also noticed (Pic 7). In the alloy modified with Mg, the oxide particles are precipitated through the whole volume of the metal matrix. The precipitation is also noticed in the regions where the largest amount of oxide is precipitated in the form of needles or small polyhedrons. Small needles and shorter lamellas have a different space orientation in face of (?) the metal surface (parallel to perpendicular). In the alloys in which the concentration of the micro-alloying element is larger than the upper critical (>0,3 mass %) or the lower critical one (<0,002 mass % of Mg), in the zone of internal oxidation, characteristic (similar to pearlite formation) orientation of oxide needles was noticed (Pic 8). The preferential precipitation of oxides along the grain boundaries, as well as grain boundaries without oxide particles were also noticed. In these alloys, a special phenomenon was noticed, namely precipitation of oxide particles in the form of letter C. This precipitation is formed at those parts of the grain boundaries where the convex side of this formation is always oriented to the surface and the Ag matrix is practically without oxide particles (Pic 9). In such an alloy, it was established that at higher temperature (850°C) passivation occurred in the whole sample. It was established that the size of oxides increases with the depth of the internal oxidation zone. In the investigated alloys with a sufficient amount of Mg, the morphological and topological features in the zone of internal oxidation were changed drastically compared to the binary alloy. In insufficiently and over-modified alloys, only some common elements with the oxidised binary alloy (such as needle, square or lamellar) oxides remained.

4 CONCLUSIONS

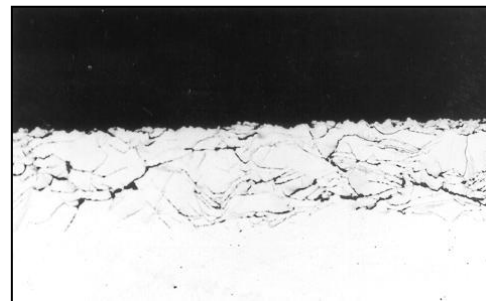
The following was established for Ag-Zn alloys with sufficient concentration of the micro-alloying element:

- The formation of shorter barriers, as well as of the main continuous oxide barriers, was prevented completely
- Small oxide particles were precipitated uniformly in the silver matrix
- In the alloys with higher concentration of Mg either some shorter oxide barriers located at a certain part of grain boundaries or oxide barriers causing passivation and hindering oxygen flow were formed

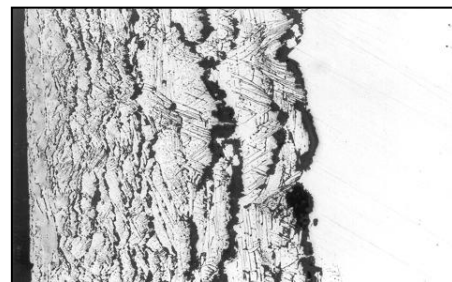
- In the alloys with lower concentration of Mg, shorter oxide barriers were formed, arranged almost parallel to the sample surface. In this way, internal oxidation was disturbed only partially because oxygen flows only from the side where oxide barriers are disconnected.



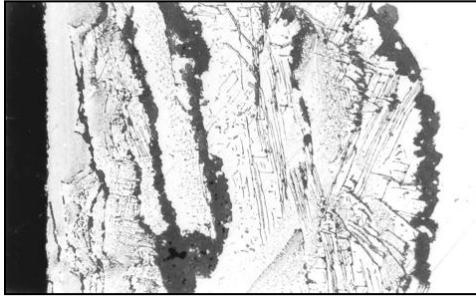
Picture 4: Characteristic shape of main oxide barrier in 2S1 alloy; 830°C, 20 hrs., air, 100 x



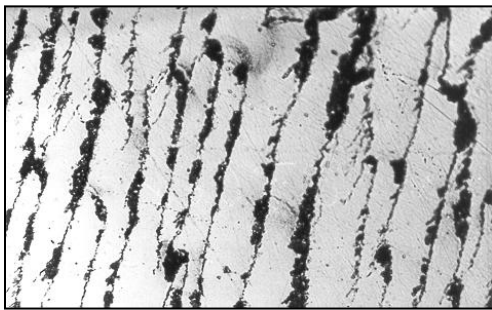
Picture 5: Preferential precipitation of oxide particles along with grain boundaries; 2S2 alloy, 750°C, 20 hrs., TGA, 100x



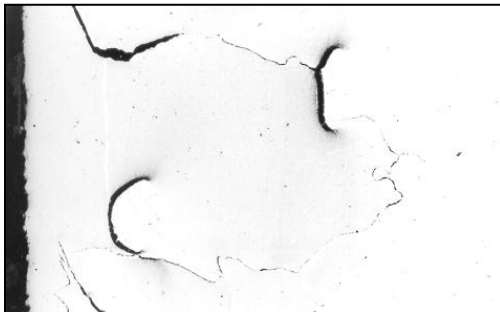
Picture 6: Shorter oxide barriers, 2S1 alloy; 800°C, 140 hrs., air, 100x, no passivation occurred



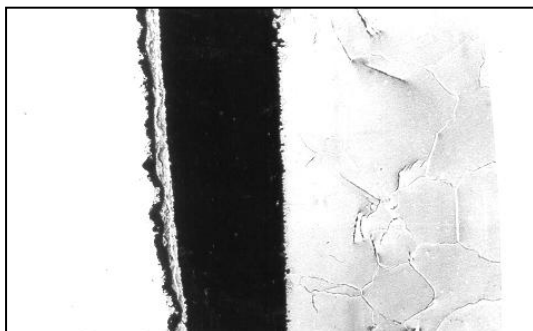
Picture 7: Shorter oxide barriers and distribution of ZnO in the form of particles and needles, 2S4 alloy modified with less than 0,002 % of Mg, 830°C, 100 hrs., air, 100×



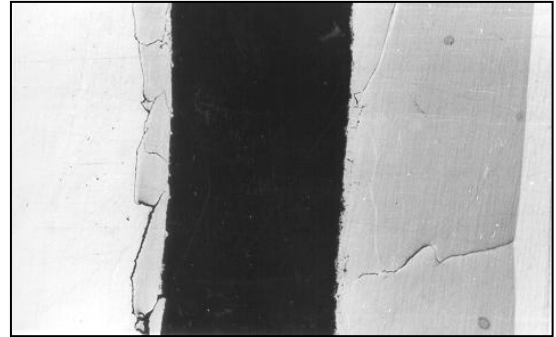
Picture 8: Preferential precipitation in the form of parallel chains in crystal grain, 2S3 alloy, 830 °C, 140 hrs., air, 500x



Picture 9: Shorter oxide barriers, 3S2 alloy, 840 °C, 20 hrs., air, 100x



Picture 10: Internal oxidation zone of 2S1 and 2S2 alloys, 830°C, 20 hrs., air, 50 ×



Picture 11: Internal oxidation zone of 3S1 and 3S2 alloys, 830°C, 20 hrs., air, 100×

It was established and proved with our investigations that the change of chemical composition of alloys, appropriate for internal oxidation, has a strong influence on the passivation process. A suitable selection of concentration of the micro-alloying element (in limits from ~ 0.002 to 0.3 mass % of Mg) can completely change the mode of internal passivation. In alloys with appropriate combination of alloying elements and a limited content of the second alloying element (up to 0.3 mass % of Mg) which is capable of forming inoculation oxides, undisturbed growth of internal oxidation zone was obtained. However, at a higher concentration of the second alloying element (above 0.3 mass % of Mg), the opposite effect (passivation) was obtained.

REFERENCES

- [1] Wagner, C. (1959): Reaktionstypen bei der Oxydation von Legierungen, Z. Elektrochem, 63, 772.
- [2] Böhm, G., (1964): Kahlwait, M.: Innere Oxydation von Metallegierungen, Acta Metall. 12, Nr.: 19, 641-648.
- [3] Stöckel, D. (1971): Kinetik der inneren Oxydation von Silber-Aluminium Legierungen, Metall, Juli, 755 - 760.
- [4] Bezjak, J. (1986): B. Sc. work, Ljubljana, Slovenia.
- [5] Bezjak, J. (1995): Ph. D. Thesis, Ljubljana, Slovenia.
- [6] Bezjak, J.: Inhibition of passivation in internally oxidised silver alloys. Z. Met.kd., 2000, letn. 91, št. 8, str. 686-691, graf. prikazi. [COBISS.SI-ID 3865673]
- [7] Bezjak, J.: TEM analyses of heterogenous nucleation of internally oxidised multi-component Ag-Zn-based alloys. Z. Met.kd., 2001, letn. 92, št. 11, str. 1253-1257, ilustr. [COBISS.SI-ID 4466505]
- [8] Metals Handbook, Metallography, Structures and Phase diagrams, September 1973, 245-257.
- [9] Bezjak, J. (1999): Passivierung in inneroxidierten Silberlegierungen, abstracted from Zeitschrift für Metallkunde. 90. (1999) 2.
- [10] R.A Rapp, D.F Frank, J.V Armitage Acta Metallurgica, Volume 12, Issue 5, May 1964, Pages 505-513
- [11] Nicholas Winograd, W. E. Baitinger, J. W. Amy and J. A. Munarin Vol. 184 no. 4136 pp. 565-567 DOI: 10.1126/science.184.4136.565
- [12] V.A van Rooijen†, E.W van Royent†, J Vrijent†, S Radelaar†, 2003.

- [13] C.P. Wu, D.Q. Yi, J. Li, L.R. Xiao, B. Wang, F. Zheng. *Journal of Alloys and Compounds*, Volume 457, Issues 1-2, 12 June 2008, Pages 565-570.
- [14] Juan F. García Martín, Sebastián Sánchez and Renaud Metz, 2011. *Kinetics Model of the Thermal Oxidation of Indium Powder*.
- [15] G. Korotcenkov, The role of morphology and crystallographic structure of metal oxides in response of conductometric- type gas sensors, *Mater. Sci. Eng. R* 61 (2008) 1-39.
- [16] E. Comini, C. Baratto, G. Faglia, M. Ferroni, A. Vomiero, G. Sberveglieri, Quasi-one dimensional metal oxide semiconductor: preparation, characterization and application as chemical sensors, *Prog. Mater. Sci.*, (In Press), Available online 10 July 2008.
- [17] A. Kolmakov, X. Chen, M. Moscovits, Functionalizing nanowires with catalytic nanoparticles for gas sensing applications, *J. Nanosci. Nanotech.* 8 (2008) 111-121.